Accepted Manuscript

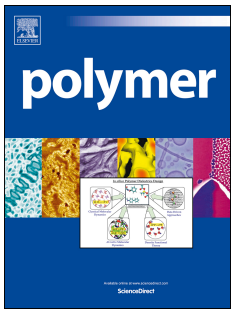

Dual Thermo- and Light-responsive Nanorods from Self-Assembly of the 4-Propoxyazobenzene-Terminated Poly(N-isopropylacrylamide) in Aqueous Solution

Xiaoqiang Xue, Jing Yang, Wenyan Huang, Hongjun Yang, Bibiao Jiang, Fang Li

PII: S0032-3861(15)30116-6

DOI: 10.1016/j.polymer.2015.07.035

Reference: JPOL 17995

To appear in: *Polymer*

Received Date: 21 April 2015

Revised Date: 27 June 2015

Accepted Date: 20 July 2015

Please cite this article as: Xue X, Yang J, Huang W, Yang H, Jiang B, Li F, Dual Thermo- and Light-responsive Nanorods from Self-Assembly of the 4-Propoxyazobenzene-Terminated Poly(N-isopropylacrylamide) in Aqueous Solution, Polymer (2015), doi: 10.1016/j.polymer.2015.07.035.

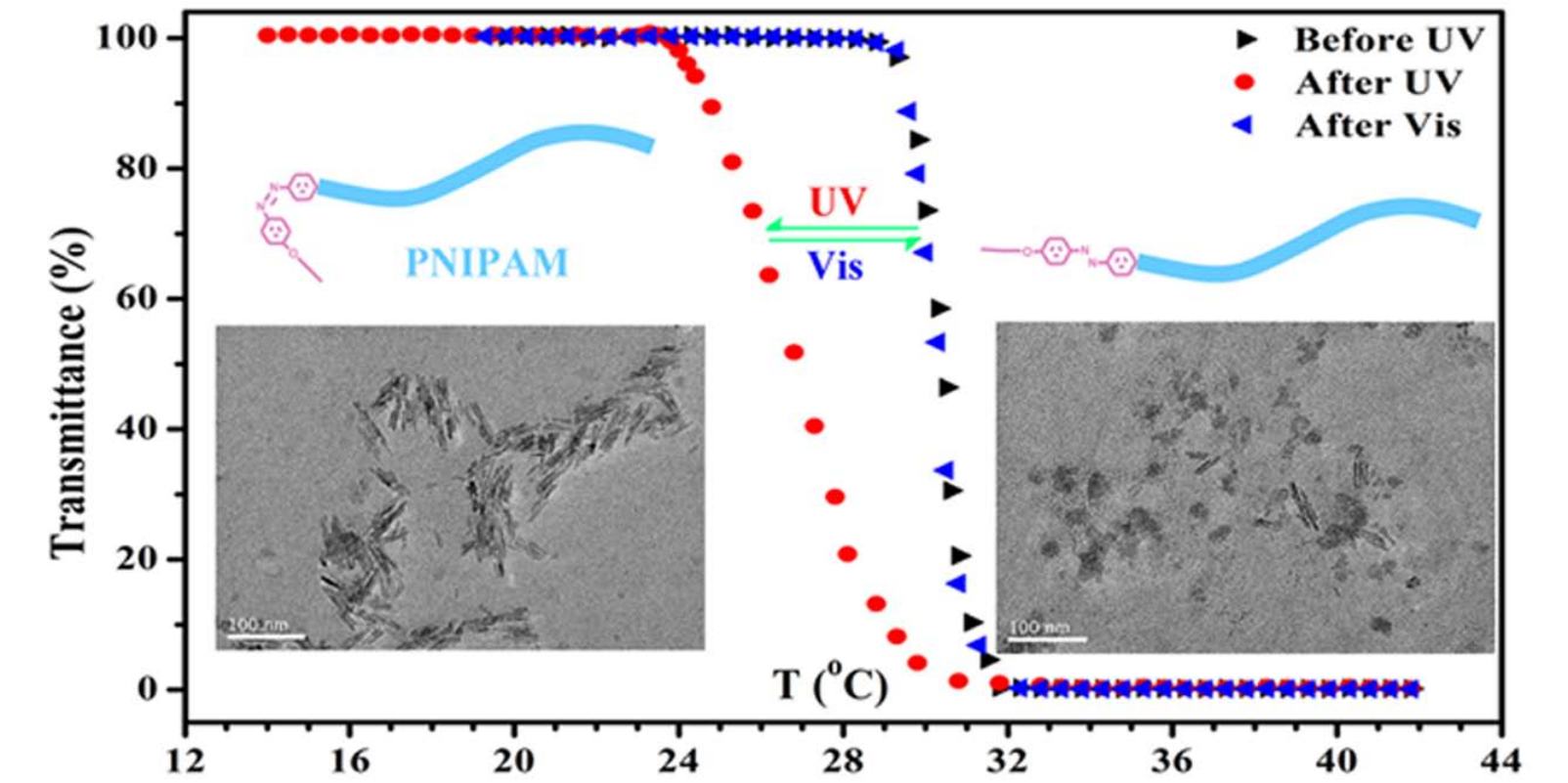
Before UV
After UV
After Vis
Transmittance (%)
T (°C)
PNIPAM
UV
Vis
100 nm
100 nm
0
20
40
60
80
100
12
16
20
24
28
32
36
40
44

Dual Thermo- and Light-responsive Nanorods from Self-Assembly of the 4-Propoxyazobenzene-Terminated Poly(*N*-isopropylacrylamide) in Aqueous Solution

Xiaoqiang Xue, Jing Yang, Wenyan Huang, Hongjun Yang, Bibiao Jiang*, Fang Li

Jiangsu Key Laboratory of Material Surface Science and Technology, School of Material Science and Engineering, Changzhou University, Changzhou, Jiangsu, 213164, People's Republic of China

*Corresponding author. Tel.: 8651986330328;

E-mail: jiangbibiao@cczu.edu.cn

Abstract Both temperature and light stimuli-responsive 4-propoxyazobenzene-terminated poly(*N*-isopropylacrylamide)s (PNIPAMs) were successfully synthesized by the atom transfer radical polymerization (ATRP) of NIPAM. ^{1}H NMR and UV-*vis* absorption spectra indicated rapid photoisomerization rate of 4-propoxyazobenzene moiety. Interestingly, the lower critical solution temperature (LCST) for PNIPAM aqueous solution clearly decreased after UV irradiation, and the repeated LCST difference (ΔT_{maxy} = 5 ^{o}C) depended on both the number-average molecular weight and amount of azobenzene chromophore. Dynamic light scattering (DLS) and static light scattering (SLS) measurements showed that the PNIPAM aqueous solution could self-assemble into nano-micelles with 4-propoxyazobenzene as the hydrophobic cores and PNIPAM chains as the hydrophilic shells. UV irradiation induced the increase of particle size due to the formation of much looser cores of *cis*-azobenzene. TEM images showed the presence of both nanorods and spherical micelles. After UV irradiation, the unstable spherical micelles transformed to metastable nanorods, then to longer rods, and finally the longer rods began to transform to flake-like particles via horizontal inter-rod aggregation above LCST.

Key words: Azobenzene polymer; Self-assembly; Stimuli-responsive.

1. Introduction

Over the past two decades, environmental stimuli-responsive polymers [1-21] to temperature, pH, light, redox, ionic strength, or electric and magnetic fields have attracted a great attention in the field of smart materials with their potential applications in controlled drug delivery [1-5], smart surfaces [6-9], biomaterials [10-12], smart sensors [13-16], and chromatographic separations [17-18]. In particular, one of the most intriguing stimuli-responsive materials is a thermo-responsive polymer which exhibits a readily accessible lower critical solution temperature (LCST) in aqueous solution. Such a thermo-responsive polymer shows a reversible hydrophilic or hydrophobic property, which can be switched by the variation of temperature. Interestingly, the LCST of poly(*N*-isopropylacrylamide) (PNIPAM) is about 32 ^{o}C, which is quite close to the human body temperature, and therefore, PNIPAM became one of the most studied thermo-responsive polymers [22-26]. Moreover, PNIPAM has been easily extended to dual- or multi- stimuli responsive polymeric materials by designing complex and well-controlled architectures [27-29], In fact, dual- or multi- stimuli responsive polymeric materials to temperature-pH [27,30,31], temperature-ionic strength [32,33], temperature-light [34,35], temperature-pH-light [36], temperature-pH-ionic strength [37-39] have been synthesized.

Recently, azobenzene compounds have gained a great deal of attention due to their unique reversible *trans-cis-trans* photoisomerization [40-42]. Thus, these polymers containing azobenzene chromophore (azobenzene polymers) are expected to be useful

for applications in optical data storage,43 holographic surface relief grating (SRG) [44-46], liquid crystal display [47,48], optical switching [49,50] and so on. Moreover, azobenzene polymers can also be used in the new area of light stimuli-responsive materials [51-54] with fascinating and advantageous properties for potential uses especially in remote activation, reversible incalculability, and in precisely controlling wavelength, illuminated area, direction, and intensity.

There have been several reports on the temperature-light responsive polymers containing azobenzene chromophore. Amphiphilic copolymers [55-63] with azobenzene located on the side-chain or main-chain can be self-assembled into nanoparticles in aqueous solution, and azobenzene groups can undergo reversible *trans-cis* photoisomerization upon UV and visible light irradiation leading to significant changes in geometry and polarity of azobenzene units. Yu and coworkers [56] reported that amphiphilic diblock copolymers were composed of ethylene oxide, azobenzene-containing methacrylate and NIPAM units, and their results showed that both temperature and light irradiation could induce a reversible change of hydrophobicity of the micellar cores. Zhao and coworkers [60] successfully synthesized poly(*N*-isopropylacrylamide) (PNIPAM) with an azobenzene-containing short segment repeatedly inserted into the main chain, which self-assembled into flower micelles at temperatures below the LCST of PNIPAM, but photoisomerization of azobenzene was found to exert little effect on the LCST.

Another exciting azobenzene-terminated PNIPAM can also be used to control the

phase transition of polymer, which was firstly published by Akiyama and Tamaoki. [64] The LCST of these polymer solutions could also be altered reversibly by light irradiation as well. Subsequently, Theato and coworkers [65] reported the synthesis of poly(oligo(ethylene glycol) methyl ether methacrylate) (P(OEGMA)) polymers with either α- or telechelic azobenzene functionalities, and there was a maximum LCST shift of 4.3 ^{o}C with light irradiation. Unusually, Jiang and coworkers [66] reported a unique amphiphilic azobenzene-containing hyperbranched poly(ether amine) (hPEA-AZO), which had a lower value of tunable cloud point (CP) after UV irradiation. The *trans* form of azobenzene was more regular, but after UV irradiation, the *trans* form of azobenzene changed into the *cis* form, and the *cis* form could not pack as closely as *trans* form in the core of hPEA211-AZO nanoparticles resulting in larger size for hPEA-AZO nanoparticles and lower value of the LCST. Chen et. Al. [67] extended the investigation of the hyperbranched poly(ethylenimine) by terminating with the azobenzene groups. In addition, they also showed that *trans* to *cis* isomerization of azobenzene units increased the CP value at pH ≈ 7, while the opposite occurred at pH ≈ 9.

The above reports indicated that the changes (increase or decrease) in the LCST of azobenzene-terminated polymers depended on both the isomerization of azobenzene and topology of the polymer. To the best of our knowledge, the effect of azobenzene structure on changes in LCST under light irradiation has not yet been investigated in detail. Akiyama and Tamaoki [64] synthesized thermo-responsive PNIPAM with the hydroxyethoxy (polarity substituent) azobenzene group at the chain end, which resulted

in the controlled LCST shift. If polarity substituent is changed into hydrophobic structure, the obtained azobenzene-terminated homopolymers in aqueous solution may self-assemble into nano-micelles, [69] which leads to the opposite changes after UV irradiation. Therefore, in this paper, we successfully synthesized the 4-propoxyazobenzene-containing initiator (4-propoxy-4′-(2-bromopropionyloxy)azobenzene, PAzo-Br) using the atom transfer radical polymerization (ATRP) of NIPAM. The unique temperature-light dual responsive behavior of the obtained 4-propoxyazobenzene-terminated polymer in water was investigated in detail, and the obtained results are presented here.

2. Experimental part

2.1. Materials.

2-Bromoisobutyryl bromide (98%; Aldrich), *p*-nitrophenol (analytical reagent; Shanghai Chemical Reagent Co. Ltd., Shanghai, China), 1-bromopropane (analytical reagent; Shanghai Chemical Reagent Co. Ltd., Shanghai, China), Nile Red (≥98%; Nanjing Oddfoni Biological Technology Co., Ltd., Nanjing, China) were used as received. *N*-isopropylacrylamide (NIPAM; 98%; Aldrich) was purified thrice by recrystallization from cyclohexane. Copper (I) chloride (CuCl; chemical pure; Shanghai Chemical Reagent Co. Ltd., Shanghai, China) was purified via washing with acetic acid and acetone, and then dried in vacuo. Tris[2-(dimethylamino)ethyl]amine (Me_6TREN) was synthesized according to the previously described procedure in the literature. [69]

Other reagents were purified using the standard procedures before use.

2.2. Characterization

Conversion of the reactants was determined using an HP-689 gas chromatography equipped with an HP-5 column (30m×0.54mm×0.5μm). Isopropyl alcohol was used as the internal standard. The carrier gas was hydrogen and the flow rate was set at 1 mL min^{-1}. The column temperature was increased from a starting value of 80 ^{o}C at sample injection to a maximum of 230 ^{o}C at 10 ^{o}C min^{-1}. The peaks were identified using chromatograms of the corresponding pure reactants. The purities of products were determined using a Waters e2695 high performance liquid chromatography (HPLC), comprising a Waters 2998 UV detector and X Bridge C18 column (5 μm, 4.6×250 mm). A mixture of acetonitrile (HPLC grade) and water (deionized and filtered with 0.45 μm membrane filter) at the gradient volume ratio (40/60~90/10~40/60) was used as the eluent. The flow rate was at 1.0 mL min^{-1} and the column temperature was 30 ^{o}C. The molecular weights ($M_{w\,GPC}$s and $M_{n\,GPC}$s) and molecular weight distributions (M_w/M_ns) of the polymers were determined with a Waters 1515 gel permeation chromatographer (GPC) equipped with a refractive index detector, using HR1, HR3, and HR4 column with molecular weights in the range of 100-500,000 g mol^{-1} which were calibrated with polystyrene (PS) standard samples. THF was used as the eluent at a flow rate of 1.0 mL min^{-1} operated at 30 ^{o}C. ^{1}H NMR spectra of the polymers were recorded on a Bruker ARX-500 type nuclear magnetic resonance instrument, using $CDCl_3$ or D_2O as solvent and tetramethyl-silane (TMS) as the internal standard. Ultraviolet visible (UV-*vis*)

absorption spectra and the transmittance at 550 nm light for lower critical solution temperature (LCST) of polymer solution (2 mg mL^{-1}) in water were performed on an Agilent Cary 100 equipped with a Cary dual cell peltier accessory (Varian). Dynamic light scattering (DLS) and static light scattering (SLS) data were acquired using an ALV/CGS-3 compact goniometer system at 25 ^{o}C, and a He-Ne laser operating at a wavelength of λ_0 = 632.8 nm was used as a light source. Sample aqueous solutions for analysis (2 mg mL^{-1}) were poured into the sample bottle, which were placed in sample cell filled with toluene used as the immersion liquid. Temperature control of the sample was provided by an external thermostated circulating bath. The accessible scattering angles range from 30 to 150°. Transmission electron microscopy (TEM) was recorded on a JEM-2100 TEM at a 100 kV accelerating voltage. Fluorescence measurements were recorded using a Cary eclipse fluorescence spectrophotometer equipped with Carry temperature controller (Agilent technologies) with a scanning rate of 600 nm min^{-1}. The excitation wavelength was 600 nm. The excitation and emission slits were 10 and 2.5 nm, respectively.

2.3. Synthesis of 4-propoxy-4'-(2-bromopropionyloxy)azobenzene (PAzo-Br)

The synthetic route of PAzo-Br is shown in Scheme S1 (see Supporting Information), and the detailed synthesis procedure and characterization are given below.

2.3.1. 1-Nitro-4-propoxybenzene

A solution of *p*-nitrophenol (5.00 g, 36.0 mmol), 1-bromopropane (3.66 g, 30.0

mmol), Na_2CO_3 (3.82 g, 36.0 mmol), and 100 mL of *N*,*N*-dimethylformamide (DMF) was added to a 250 mL round bottom flask under vigorous stirring. The solution was stirred under reflux at 140 ^oC for 6 h. After cooling to room temperature, the mixture was poured into 200 mL of water under vigorous stirring. The crude product was extracted with dichloromethane (50 mL) and washed with 5% Na_2CO_3 aqueous solution and deionized water three times. The organic layer was dried with anhydrous $MgSO_4$ overnight, filtered and evaporated under reduced pressure. The pure 1-nitro-4-propoxybenzene (3.92 g, yield: 72.2%) was obtained as yellow liquid. The purity was 93.5% (HPLC). ^1H NMR (400MHz, $CDCl_3$), δ (TMS, ppm): 8.13-8.22 (m, 2H, ArH), 6.87-6.97(m, 2H, ArH), 3.95-4.05 (t, 2H, CH_2O), 1.77-1.90 (m, 2H, CH_2), 0.99-1.10 (t, 3H, CH_3).

2.3.2. 4-Propoxyaniline

A mixture of iron powder (1.15 g, 30.0 mmol) and NH_4Cl salt (2.65 g, 50.0 mmol) in 50 mL of distilled water was prepared in a 500 mL flask under vigorous stirring. Then, a 100 mL methanolic solution (3.62 g, 20.0 mmol) was added dropwise into this mixture over 10 min at room temperature. The resultant mixture was stirred under gentle reflux for 5 h. After raising the room temperature, the inorganic residue was filtered, and the methanol was evaporated under vacuum. The mixture was extracted with ethyl acetate (50 mL) and washed with deionized water (90 mL) three times. The organic layer was dried with anhydrous $MgSO_4$ overnight, filtered and evaporated under reduced pressure. The final crude 4-propoxyaniline (2.60 g) was stored in dark condition.

2.3.3. 4-Propoxy-4′-hydroxyazobenzene

The crude 4-propoxyaniline (2.60 g, about 16.0 mmol) was dissolved in concentrated HCl (5 mL) and deionized water (15 mL). The mixture prepared by stirring at 0-5 ^{o}C in an ice bath, and then aqueous solution (2 mL) of $NaNO_2$ (1.24 g, 18.0 mmol) was added slowly. A yellow transparent diazonium salt solution was stirred at 0-5 ^{o}C for 30 min. A coupling solution of phenol (1.88 g, 20.0 mmol), Na_2CO_3 (3.18 g, 30.0 mmol), $NaHCO_3$ (2.52 g, 30.0 mmol) and deionized water (50 mL) was cooled to 0 ^{o}C. Then the diazonium salt solution was added dropwise to the coupling solution at a temperature range of 0-5 ^{o}C. The pH of the mixture was adjusted to 8~9 using a 40% NaOH solution, and the mixture was further stirred for 5 h at 0-5 ^{o}C. A red-orange precipitate was collected by filtration, washed with deionized water several times, and dried under vacuum. The crude products were recrystallized three times from ethanol to achieve pure 4-propoxy-4′-hydroxyazobenzene as red-orange crystal (3.30 g, yield: 81.2%). The purity was 95.8% (HPLC). ^{1}H NMR (400MHz, $CDCl_3$), δ (TMS, ppm): 7.76-7.89 (m, 4H, ArH), 6.96-7.01 (d, 2H, ArH), 6.88-6.95 (d, 2H, ArH), 3.96-4.04 (t, 2H, CH_2O), 1.77-1.91 (m, 2H, CH_2), 1.00-1.10 (t, 3H, CH_3).

2.3.4. PAzo-Br

4-Propoxy-4′-hydroxyazobenzene (3.07 g, 12.0 mmol), freshly distilled triethylamine (1.52 g, 15.0 mmol) and freshly distilled THF (50 mL) were added to a 250 mL three-necked flask. The solution was stirred in an ice bath. 2-Bromoisobutyryl bromide (1.85 mL, 15.0 mmol) diluted in dry THF (20 mL) was then added to the cool

stirred mixture dropwise. The reaction mixture was vigorously stirred for 5 h at 0-5 ^{o}C and then at room temperature overnight. The mixture was filtered, and the filtrate was evaporated under vacuum. The remaining yellow mixture was dissolved in ethyl acetate and washed with 5% Na_2CO_3 aqueous solution and deionized water three times, dried with anhydrous $MgSO_4$ overnight, filtered and evaporated under reduced pressure. The final crude product was recrystallized three times from ethanol to yield yellow solid (3.12 g, yield: 64.2%). The purity was above 98% (HPLC). ^{1}H NMR (400MHz, $CDCl_3$), δ (TMS, ppm): 7.85-8.00 (m, 4H, ArH), 7.22-7.32 (d, 2H, ArH), 6.97-7.05 (d, 2H, ArH), 3.96-4.06 (t, 2H, CH_2O), 2.10 (s, 6H, $C(CH_3)_2$), 1.79-1.91 (m, 2H, CH_2), 1.02-1.11 (t, 3H, CH_3) (^{1}H NMR spectrum was provided in Supporting Information, Figure S1).

2.4. General procedure for the 4-propoxyazobenzene-terminated poly(N-isopropylacrylamide) (PNIPAM1~PNIPAM7) using PAzo-Br

Me_6TREN (0.230 g, 1.00 mmol), CuCl (0.033 g, 0.33 mmol), isopropyl alcohol (3.00 g) and water (1.00 g) were added to a 25 mL Schlenk flask equipped with a stir bar. The flask was cycled between vacuum and argon (3 times) in an ice bath, and the solution was stirred for 30 min. PAzo-Br (0.135 g, 0.33 mmol) and NIPAM (1.13 g, 10.00 mmol) were added to the reaction vessel. After three freeze-pump-thaw cycles, the flask was placed in an oil bath to start the polymerization at 25 ^{o}C. After a preset reaction time, the polymerization was stopped by adding $CuBr_2$ (0.074 g, 0.33 mmol). After solvent evaporation, the crude polymers were dissolved in about 10 mL THF, passed through a small neutral Al_2O_3 chromatographic column to remove Cu^{2+} deactivator, and

precipitated by dropwise addition to cold hexane (200 mL). The precipitates were filtrated. The obtained polymers were redissolved in THF, isolated by precipitation into hexane, and dried to a constant weight at room temperature in vacuum. The other polymers were prepared using similar procedures. All the polymers were dissolved in THF and filtered by PTFE film for GPC analysis. The samples were dissolved in $CDCl_3$, and measured by ^1H NMR spectroscopy.

3. Results and discussion

3.1. Synthesis of the 4-propoxyazobenzene-terminated poly(N-isopropylacrylamide) (PNIPAMs) via the atom transfer radical polymerization (ATRP)

The synthesis route is shown in Scheme 1, and the detailed discussion of PNIPAMs were provided in Supporting Information.

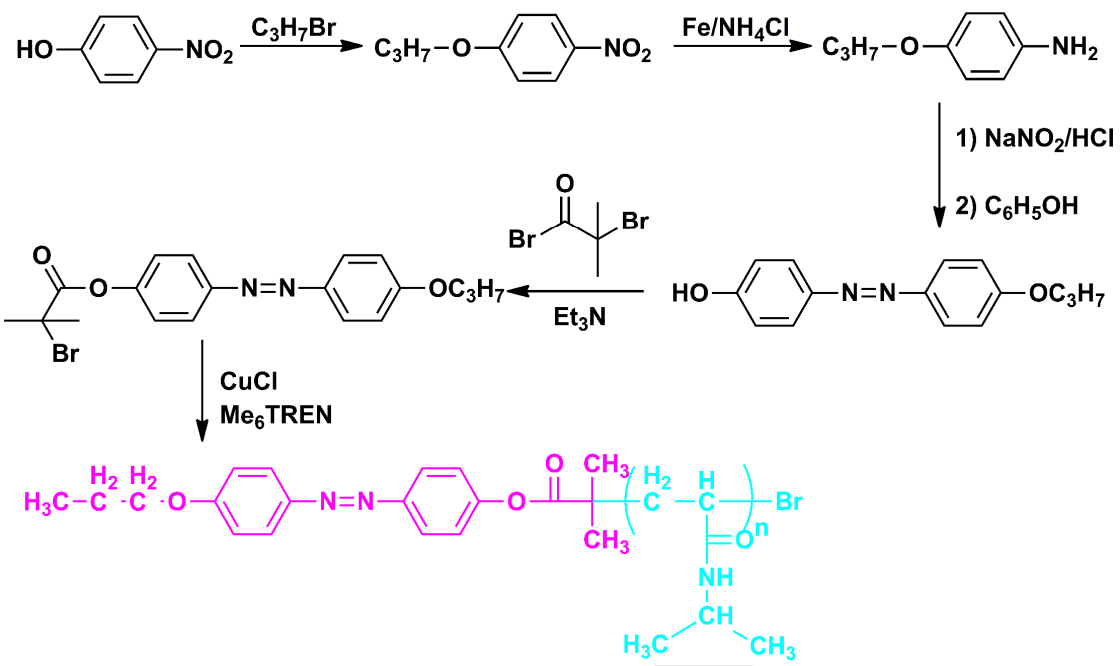

Scheme 1. Synthetic Route of the 4-propoxyazobenzene-terminated poly(*N*-isopropylacrylamide) (PNIPAM).

3.2. Photoisomerization behavior of 4-propoxyazobenzene-terminated PNIPAM

Azobenzene compounds exhibited photoisomerization behavior, which undergoes reversible conversion between *trans*- and *cis*- form under the irradiation of UV and visible light. Closer inspection of the ^{1}H NMR spectra of PNIPAM4 (Figure 1) could provide a powerful line of evidence about *trans-cis* form variation of azobenzene at the end of the polymer after UV irradiation. As shown in Figure 1, the weak signals at around 7.82-7.98 ppm (a in Figure 1) due to phenyl protons of the *trans*-form azobenzene group were mostly shifted upfield resulting in two peaks at 6.85-6.98 ppm and 6.71-6.81 ppm (a' in Figure 1) relative to the *cis*- form under only 5 min UV irradiation (365 nm). Meanwhile, a new resonance signal at 3.92 ppm (b in Figure 1)

appeared and should be assigned to methylene protons from the terminal 4-propoxyazobenzene, which were overlapped by the methenyl protons of the NIPAM units before UV irradiation. However, after a prolonged UV irradiation (15 and 30 min), the *trans*-form of the azobenzene did not completely disappear, which indicated the incomplete photoisomerization, and content of *trans*-form azobenzene (x_{trans}) was still only 25% according to the integrals calculated by eq 1.

$$x_{trans} = \frac{I_{7.82\text{ - }7.98}}{I_{7.82\text{ - }7.98} + I_{6.85\text{ - }6.98} + I_{6.71\text{ - }6.81}} \times 100\% \qquad (1)$$

Where, $I_{7.82\text{-}7.98}$, $I_{6.85\text{-}6.98}$ and $I_{6.71\text{-}6.81}$ were the integrals of the signals at 7.82-7.98 ppm, 6.85-6.98 ppm and 6.71-6.81 ppm in Figure 1 (B), respectively.

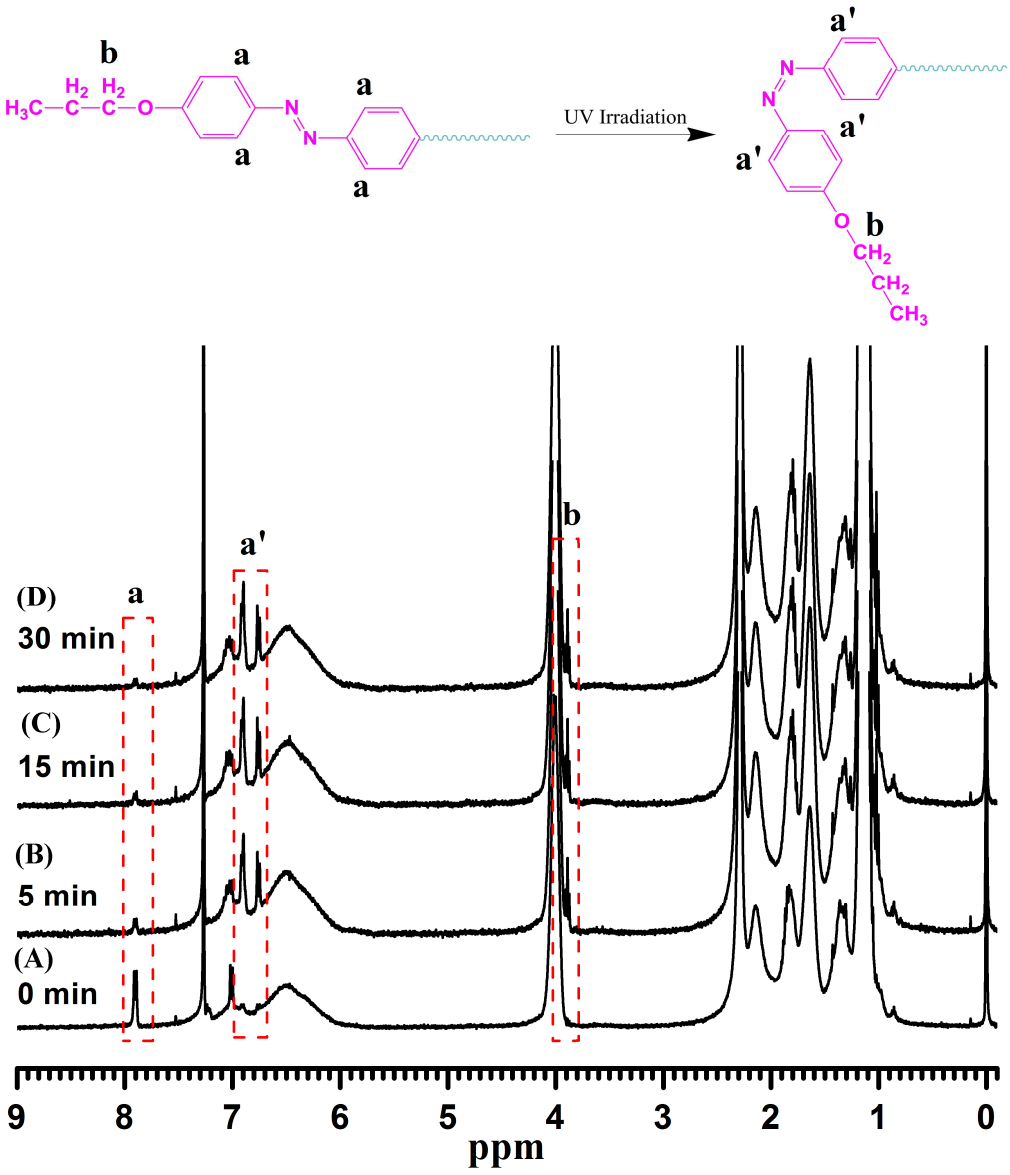

Figure 1. ^{1}H NMR spectra of the PNIPAM4 ($M_{n\,GPC}$ = 5300 g mol^{-1}, M_w/M_n = 1.16) in $CDCl_3$ under irradiation of 365 nm UV light for 0 min (A); 5 min (B); 15 min (C); 30 min (D).

In addition, the UV-*vis* absorption spectra of PNIPAM4 in $CHCl_3$ solution were recorded at different time intervals of UV irradiation until photostationary state was reached (Figure 2 (A)). Upon UV irradiation (365 nm), the maximum absorption at about

350 nm corresponding to the π-π* transition of *trans* azobenzene in polymer decreased rapidly.[70] Meanwhile, the weak n-π* transition band of the *cis* form azobenzene at about 440 nm slightly increased with the irradiation time. The *trans*-form of the azobenzene did not completely disappear as there was about 27% *trans*-form of azobenzene, which was consistent with the results determined by ^{1}H NMR spectra of PNIPAM4. Interestingly, there were only 30 s to reach photostationary state, and the *trans-cis* isomerization rate of PNIPAM4 was very fast. On the other hand, *cis-trans* isomerization of the irradiated PNIPAM4 could also be achieved by visible light irradiation. As shown in Figure 2 (B), the absorption of *trans* azobenzene at 350 nm was restored to the initial state of PNIPAM4 in 1000 s as same as the absorption of *cis* form, which showed the equilibrium between *cis* and *trans* forms was completely established. This result confirmed that the rapid photoisomerization of azobenzene in the end of PNIPAM was reversible between the UV and visible light irradiation, which could have an appealing application in light stimuli-responsive material.

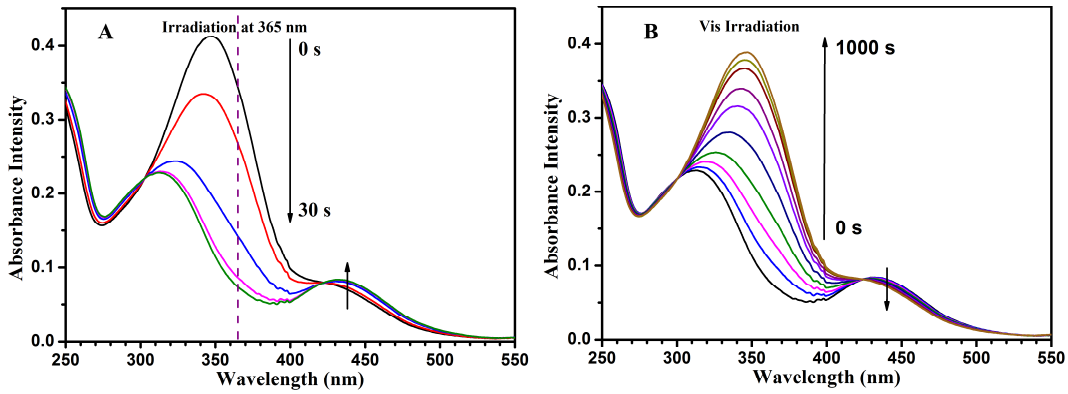

Figure 2. Evolution of UV-*vis* absorption spectra of the polymer PNIPAM4 ($M_{n\,GPC}$ = 5300 g mol^{-1}, M_w/M_n = 1.16) aqueous solution prepared under different time intervals in $CHCl_3$ (The concentration of solution is 2 mg mL^{-1}) at room temperature with UV light of 365 nm (A) and further visible light (B) irradiation.

3.3. The response of 4-propoxyazobenzene-terminated PNIPAMs to temperature and light

It is well-known that PNIPAM is a widely investigated thermo-responsive polymer, which exhibits reversible drastic phase-transition at its lower critical solution temperature (LCST) around 32 ^{o}C. The introduction of the hydrophilic or hydrophobic moiety into the PNIPAM chain would appreciably increase or decrease the LCST of the corresponding polymer in a characteristic manner. On the basis of this valuable behavior of PNIPAM, we successfully introduced a dual-stimuli responsive PNIPAM terminated with the hydrophobic 4-propoxyazobenzene moiety, and then studied temperature dependence of the 550 nm optical transmittance to measure the changes of LCSTs of the PNIPAM aqueous solution (2 mg mL^{-1}) before and after UV (365 nm) and further visible light irradiation. These results are presented in Figure 3 (A). The transmittance of PNIPAM4 solution remained almost constant below 29 ^{o}□C, and the sharp decrease of transmittance above 29 ^{o}□C means phase separation without precipitation. The LCSTs of PNIPAMs ended with 4-propoxyazobenzene as listed in Table S1 (see the Supporting Information) were lower than the normal value (about □32 ^{o}□C), which was due to the hydrophobicity of azobenzene structure [64]. Moreover, this process under the alternating temperature of 25 ^{o}C and 35 ^{o}C was reversible and repeatable at least 5 cycles

without any change of transmittance, as shown in Figure S4 (see the Supporting Information). By the incorporation of 4-propoxyazobenzene in the end of PNIPAM, the LCST would be influenced by the photoisomerization of azobenzene [64,65]. Surprisingly, when the PNIPAM4 solution was exposed to UV light at 365 nm for 5 min, the *trans-cis* photoisomerization reaction had completed a photostationary state, and there was a significant decrease (~5 ^{o}C) of the LCST value (~24 ^{o}C) compared with that of the initial state (~29 ^{o}C). This result is different from the previously reports about linear PNIPAM containing azobenzene group [64,65]. Moreover, the transmittance decreased thereafter with accompanied by expanding temperature range of the transition, which was consistent with the previously reports due to inhomogeneity in the polymer [71]. The LCST downshift (ΔT) of the irradiated PNIPAM4 solution could be also restored to the initial temperature under the further exposure of visible light (Figure 3(A)), and the LCST differences between irradiated and nonirradiated solution were affected by amount of azobenzene chromophore [63-65] of PNIPAM. It is interesting to note that in Figure 3 (B), and the LCST downshifts increased, as expected, from 1.9 to 5.0 ^{o}□C with the increase of $M_{n\,GPC}$ from 3100 to 5300 g mol^{-1}, following decrease with the decreasing amount of azobenzene chromophore. The results thus showed that the LCST downshifts of 4-propoxyazobenzene-terminated PNIPAM depended on both the $M_{n\,GPC}$ and amount of azobenzene chromophore. Interestingly, this material might be well used for the light-responsive trigger switch of the phase transition with the large temperature range. Figure 4 showed the changes in transmittance of PNIPAM4 solution

(2 mg mL^{-1}) irradiated with alternating UV and visible light at 28 ^{o}C. The transmittance between 99% and 12% was reversibly switched by the tuning of external conditions of UV light and visible light irradiation, which indicated that the phase transition of the PNIPAM ended with 4-propoxyazobenzene could be reversibly controlled by light.

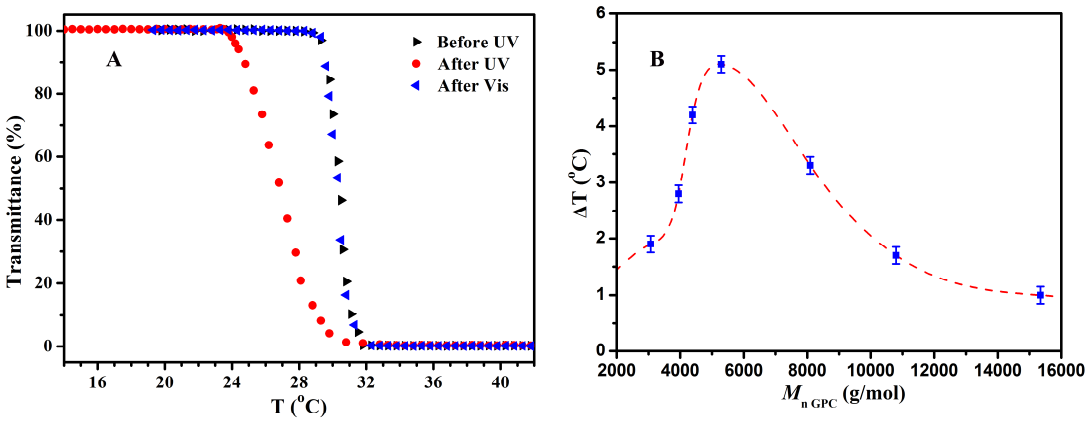

Figure 3. (A) Temperature dependence of the transmittance at 550 nm light through a 2 mg mL^{-1} PNIPAM4 ($M_{n\,GPC}$ = 5300 g mol^{-1}, M_w/M_n = 1.16) aqueous solution; (B) Lower critical solution temperature (LCST) downshifts (ΔT) of PNIPAMs plotted as a function of the molecular weights ($M_{n\,GPC}$s) of PNIPAMs.

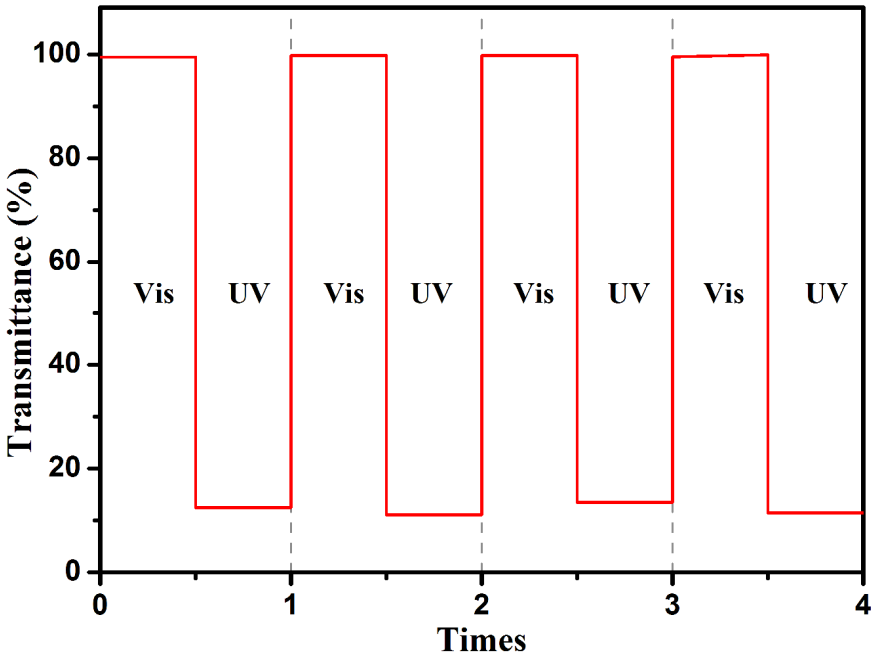

Figure 4. Reversible changes of transmittance at 550 nm for the PNIPAM4 ($M_{n\,GPC}$ = 5300 g/mol, M_w/M_n = 1.16) aqueous solution (2 mg mL^{-1}) at 28 °C under alternating irradiation of UV and visible light.

Generally speaking, the LCST of PNIPAM functionalized with azobenzene units could shift in polymer water solution response upon exposure to UV light [63-65,71], which was due to the higher polarity of *cis*-form than *trans*-form azobenzene. However, when the terminated azobenzene in PNIPAM was designed to hydrophobic 4-propoxyazobenzene, the results were the opposite. This 4-propoxyazobenzene-terminated PNIPAM aqueous solution could self-assemble into nano-micelles [68], and UV irradiation induced changes to the aggregate micelles with the result of the LCST downshift [66]. Therefore, the transition temperature of PNIPAM4 solution by measuring the transmittance could not accurately reflect the LCST of the isolated polymer chains, and it displayed the solution of the aggregates. The

change in the transmission was caused by the aggregation of the self-assembled structures. The LCST of PNIPAM4 solution could be determined by ^{1}H NMR spectra in D_2O (Micro-THF as the internal standard) with the different temperature before and after UV irradiation. As shown in Figure 5 (A), the weak signals at around 7.82-7.98 ppm (b) due to phenyl protons of the *trans*-form azobenzene group before UV irradiation decreased rapidly as the temperature increased, which was due to the closer cores of *trans*-azobenzene from the hydrophobic conversion of the PNIPAM chains. When the temperature was up to 31 ^{o}C, phenyl proton signals disappeared, which demonstrated that the isolated polymer chains got together via the hydrophobic conversion. After UV irradiation, the phenyl proton signals of the *trans*-form azobenzene were mostly shifted upfield at 6.57-7.15 ppm relative to the *cis*-form. The most important point was that phenyl proton signals disappeared at the lower temperature (29 ^{o}C), and the LCST of PNIPAM solution decreased after UV irradiation. In order to determine the LCST of PNIPAM4 solution, the relative integrals (THF integrals as the internal standard at 3.70-3.80 ppm) of the signals at 7.82-7.98 ppm (a) had been traced on line at the different temperature in Figure 5, and the results was shown in Figure 6. It is also clear from Figure 6 that the LCST of PNIPAM4 solution was about 25 ^{o}C before UV irradiation, and 28 ^{o}C after UV irradiation, respectively, and these results accorded with the experiments by measuring the transmittance.

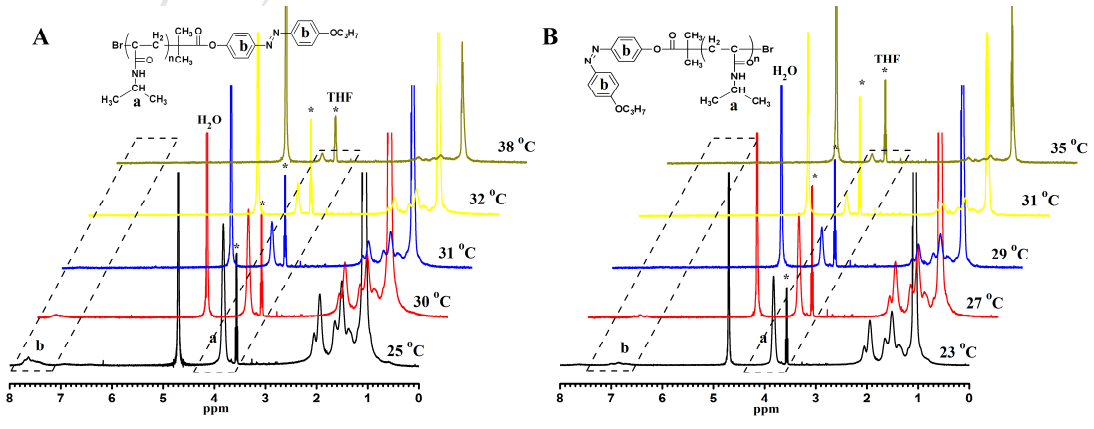

Figure 5. ^{1}H NMR spectra of the 2 mg mL^{-1} PNIPAM4 ($M_{n\,GPC}$ = 5300 g mol^{-1}, M_w/M_n = 1.16) solution in D_2O (Micro-THF as the internal standard) with the different temperature. A: Before UV irradiation; B: After UV irradiation for 30 min.

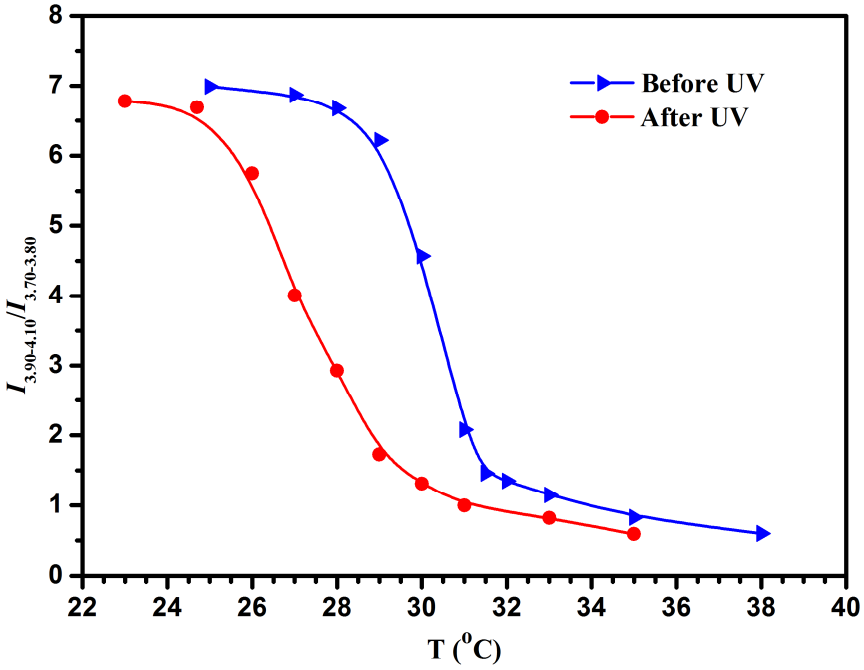

Figure 6. Temperature dependence of $I_{3.90\text{-}4.10}/I_{3.70\text{-}3.80}$ through a 2 mg mL^{-1} PNIPAM4 ($M_{n\,GPC}$ = 5300 g mol^{-1}, M_w/M_n = 1.16) aqueous solution, $I_{3.90\text{-}4.10}$ and $I_{3.70\text{-}3.80}$ were the integrals of the signals at 3.90-4.10 ppm and 3.70-3.80 ppm in ^{1}H NMR spectra of the PNIPAM4 (Figure 5).

In order to understand why the photoisomerization of azobenzene could downshift the LCST of the 4-propoxyazobenzene-terminated PNIPAM aqueous solution, we conducted detailed experiments with the light-responsive self-assembly behavior of polymer solution by dynamic light scattering (DLS) and static light scattering (SLS)

measurements simultaneously as shown in Figure 7 (A and B). Figure 7 (A) showed intensity-weighted size distributions of R_h for the PNIPAM4 solution before UV irradiation (23 and 25 ^oC) and after UV irradiation (23, 23.6 and 24 ^oC). DLS measurements indicated that sample PNIPAM4 formed a rather broad size distribution of micelles with an average intensity-weighted size of about 17 nm, which remained stable at 23 and 25 ^oC. These results showed that the particles were composed of the hydrophobic core (terminated 4-propoxyazobenzene) and the hydrophilic shell (PNIPAM chains) in amphiphilic homopolymer (PNIPAM4) [68]. Due to both *tran*- and *cis*-azobenzene in the initial state, these micelles contained some larger particles, which were in exist with complex morphology as revealed by the tailing peak. After UV irradiation, the R_h of the PNIPAM4 solution increased to 29 nm, and the size distribution developed into bimodal distribution with much wider, which indicated the PNIPAM4 further self-assembled to generate the larger micelles. The hydrophilic PNIPAM chains transformed to hydrophobic chains by heating. The collapsed micelles became unstable and assemble together as multiple larger particles. Moreover, R_h increased significantly to 70 and 106 nm with raising temperature (23.6 and 24 ^oC), and the bimodal distribution was rapidly changed into trimodal and multimodal type, which suggests that UV irradiation induced changes to the aggregate micelles with a faster thermo-response.

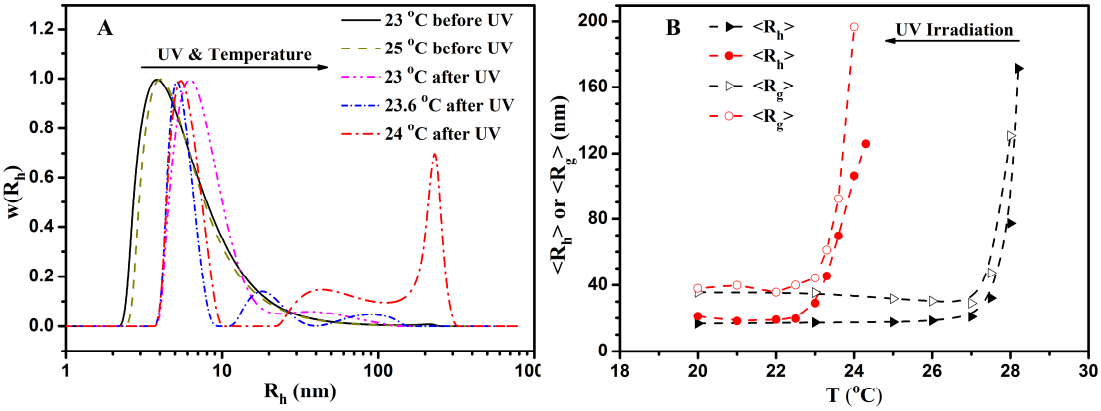

Figure 7. (A) Intensity-weighted size distributions of the hydrodynamic radius (R_h) obtained by dynamic light scattering (DLS) for a 2 mg mL^{-1} PNIPAM4 ($M_{n\,GPC}$ = 5300 g mol^{-1}, M_w/M_n = 1.16) aqueous solution measured before UV irradiation; (B) Temperature dependence of average radius of gyration (<R_g>) and average hydrodynamic radius (<R_h>) of the PNIPAM4 aqueous solution.

On the other hand, SLS measurements at several angles were extrapolated in a *Zimm* plot, and self-assembly properties were further calculated in Figure 7 (B). Figure 7 (B) shows temperature dependence of average radius of gyration (<R_g>) and average hydrodynamic radius (<R_h>) of the PNIPAM4 solution obtained from SLS and DLS measurements, respectively. When the solution was heated to 27.0 °C, there was a stably aggregate size (<R_g> = 32 nm,), but <R_h> dropped slowly due to regional shrinkage of the PNIPAM chains. An abrupt increase of the PNIPAM4 solution was observed above 27.0 °C, which verified the LCST behavior and also displayed narrow gaps with optical transmittance tests (29.0 °C) due to instrumental errors. These results further confirmed the micellar aggregation. Both of <R_g> and <R_h> unobtrusively changed before and after irradiation below 22.5 °C. When the temperature would have continued rising, the

particles size began to grow after UV irradiation, and $<R_g>$ was 35.8 nm at 22 ^oC, 40 nm at 22.5 ^oC, 44 nm at 23 ^oC, and so on. Therefore, UV irradiation induced not only increase of particle size above 22.5 ^oC, but also led to a decrease of the LCST (22.5 ^oC). The hydrophobic core of the nanostructured micelles was 4-propoxyazobenzene attached to the end of PNIPAM. Before UV irradiation, *trans* form of azobenzene had a regular structure, and PNIPAM4 solution formed the tight cores of *trans*-azobenzene in an ordered array. When PNIPAM4 solution was irradiated by UV light, the *cis* form packed to the loose cores with the disordered array in the PNIPAM4 nanoparticles, resulting in the increase of the size of the micelles [66]. With a further increase in temperature, the loose cores from the *cis* form azobenzene became unstable and formed the much larger micelles due to the coiled PNIPAM chains.

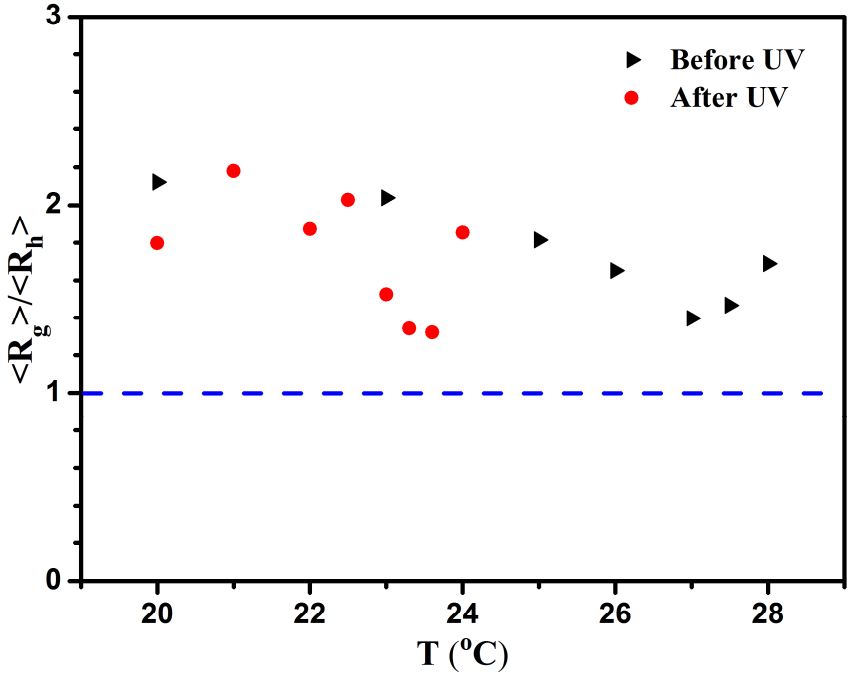

Figure 8. Ratio of average radius of gyration (<R_g>) and average hydrodynamic radius (<R_h>) for a 2 mg mL^{-1} PNIPAM4 ($M_{n\,GPC}$ = 5300 g mol^{-1}, M_w/M_n = 1.16) aqueous solution at different temperatures.

To get an insight into the morphology of the micelles, the ratio (<R_g>/<R_h>) of average radius of gyration (<R_g>) and average hydrodynamic radius (<R_h>) could be characterized by the aggregate particle shape and chain density distribution. Ordinarily, <R_g>/<R_h> value could be attributed to spheres (<R_g>/<R_h> < 1) [72], vesicles (<R_g>/<R_h> ≈ 1)[73] and rods (<R_g>/<R_h> > 1) [74]. Figure 8 shows the temperature dependence of the <R_g>/<R_h> value for PNIPAM4 aqueous solution before and after UV irradiation. All the <R_g>/<R_h> values in the interval 1.3-2.1 were attributed to the

rod-like micelles. Before UV irradiation, the $<R_g>/<R_h>$ values of the micelles gradually decreased from 2.1 to 1.4 with raising temperature below LCST, while both the $<R_g>$ and $<R_h>$ decreased a little as shown in Figure 7 (B), because of intrachain contraction of thermo-responsive PNIPAM chains.[75] The lower value of $<R_g>/<R_h>$ further confirmed that the collapsed PNIPAM chain became the denser shell in the core-shell micelle. After UV irradiation, the $<R_g>/<R_h>$ values rapidly decreased from 2.0 to 1.3 in the narrow temperature range of 22-24 ^{o}C, further indicating the much faster temperature sensitivity of the rod-like micelles compared with the unirradiated solution. When the temperature of PNIPAM4 aqueous solution reached LCST (T = 24 ^{o}C), the $<R_g>/<R_h>$ value was close to 2, which indicated the conformation change of aggregate PNIPAM particles.

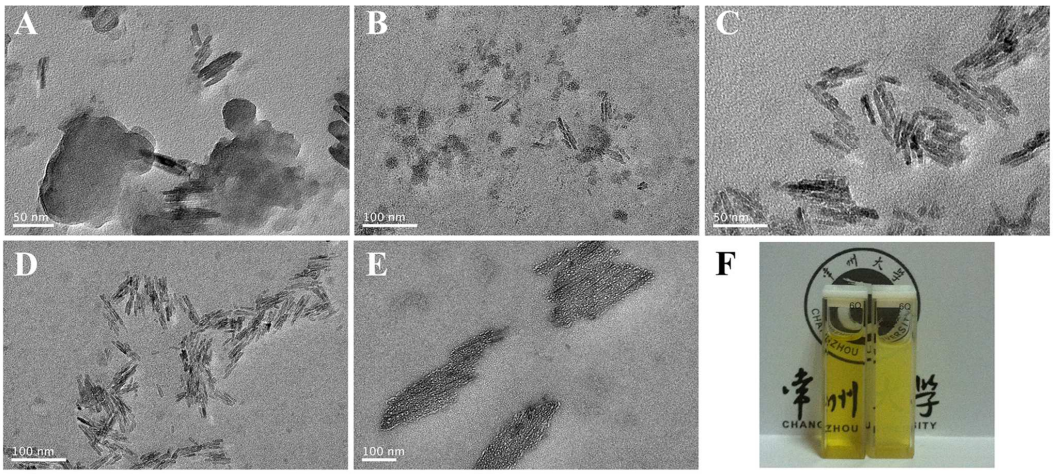

Figure 9. Transmission electron micrographs (TEMs) of aggregates formed in the PNIPAM4 ($M_{n\,GPC}$ = 5300 g mol^{-1}, M_w/M_n = 1.16) aqueous solution (2 mg mL^{-1}) at different temperature before (A: 23 ^{o}C; B :24 ^{o}C) and after irradiation with UV light (C: 23 ^{o}C; D: 24 ^{o}C and E: 26 ^{o}C). F: Images of the PNIPAM4 solution before (left) and after irradiation with UV light (right).

To further gain direct information about the rod-like micelles, typical transmission electron micrographs (TEMs) in Figure 9 could directly exhibit the overall shape of the particles. Before UV irradiation, Figure 9 (A) and (B) revealed the presence of both rods (about 10-80 nm in length) and spherical micelles (about 25-100 nm in diameter) with rather broad size distribution, which is close to the R_h of particles in solution obtained by DLS analysis. Therefore, the $<R_g>/<R_h>$ (above 1) of the rods was an average value, and the particles with rod-like morphology were predominant in PNIPAM4 solution at 24 ^oC (Figure 9 (B)). During UV irradiation, spherical micelles disappeared with the whole range of temperature (Figure 9 (C)), and the rods continued to grow longitudinally with increasing temperature (Figure 9 (D)). It is likely that the hydrophobic *trans*-form of the azobenzene transformed into the strong polar *cis*-form, which then induced conversion from the unstable spheres to metastable rod-like micelles, along with the formation of much looser cores from *cis*-azobenzene. Moreover, heating made the hydrophilic PNIPAM shells shrink to rods with half width, and the two collapsed rods gather together as the longer rods keeping the constant width (Scheme 2), which also confirmed the collapsed PNIPAM chain became a denser shell in the core-shell micelle. When the temperature increased to 26 ^oC (higher than LCST), the longer rods began to transform as the flake particles via horizontal inter-rod aggregation (Figure 9 (E)), which could be attributed to the formed hydrophobic PNIPAM chains. Therefore, micelles self-assembled by the 4-propoxyazobenzene-terminated PNIPAMs could be triggered to

form the larger particles with much more thermo-response by UV irradiation leading to the LCST downshift.

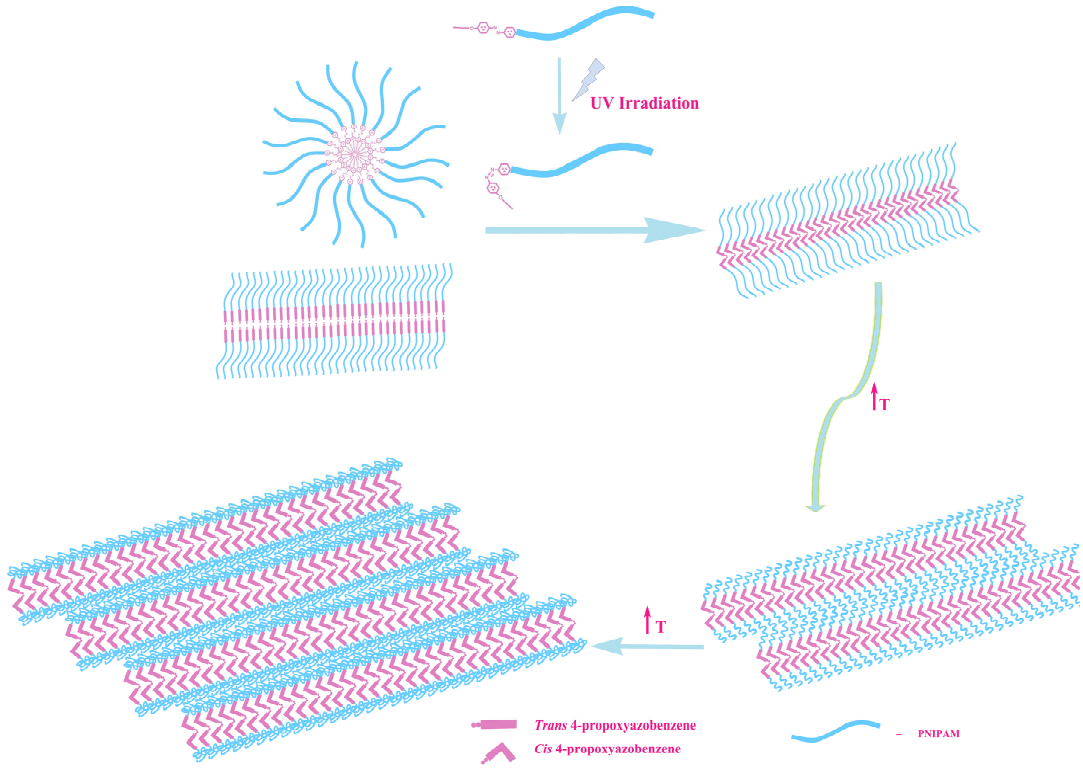

Scheme 2. The formation mechanism of the flake particles for the PNIPAM4 ($M_{n\,GPC}$ = 5300 g mol^{-1}, M_w/M_n = 1.16) aqueous solution (2 mg mL^{-1}).

4. Conclusions

In summary, we have presented the synthesis of 4-propoxyazobenzene-terminated poly(*N*-isopropylacrylamide)s (PNIPAMs) with different molecular weights (3000~15000 g mol^{-1}) and narrow molecular weight distributions (M_w/M_n < 1.35) via the atom transfer radical polymerization (ATRP) of *N*-isopropylacrylamide (NIPAM) using 4-propoxy-4′-(2-bromopropionyloxy)azobenzene (PAzo-Br) as the initiator. 4-Propoxyazobenzene at the end of PNIPAM exhibited rapid photoisomeriztion rate, and this transformation process between *trans*- and *cis*- form was reversible and repeatable under the alternating irradiation of UV and visible light. Interestingly, the lower critical solution temperature (LCST) of PNIPAM aqueous solution after UV irradiation was lower than that before UV irradiation, and the repeatable LCST downshifts (*e.g.* ΔT_{max} = 5 ^{o}C corresponding to PNIPAM4) was achieved through the irradiation of light, which depended on both the number-average molecular weight ($M_{n\ GPC}$) and amount of azobenzene chromophore. Before UV irradiation, the PNIPAM aqueous solution could self-assemble into nano-micelles with the hydrophobic cores (terminated 4-propoxyazobenzene) and the hydrophilic shells (PNIPAM chain). There were both rods and spherical micelles in the PNIPAM aqueous solution. Dynamic light scattering (DLS), static light scattering (SLS) and transmission electron micrograph (TEM) measurements indicated that the micelles had rather broad size distribution with an average intensity-weighted size of about 17 nm. UV irradiation induced the increase of particle size due to the formation of much looser cores from *cis*-azobenzene. Simultaneously, the

unstable spherical micelles transformed to metastable rod-like micelles, and the heating made the hydrophilic PNIPAM shells shrink to rods with half width, which gather together as the longer rods. Then, the longer rods began to transform to flake-like particles via horizontal inter-rod aggregation above LCST. Therefore, micelles could be triggered to form the larger particles with much more thermo-response by UV irradiation, which led to the LCST downshift.

Supporting Information.

^{1}H NMR spectra of PAzo-Br and PNIPAM4; Characteristic data for PNIPAMs; GPC curves of PNIPAMs; Reversible changes of transmittance at 550 nm for the PNIPAM aqueous solution

Acknowledgements

The financial support of this work by the National Natural Science Foundation of China (Nos. 21104006), a project funded by the Priority Academic Program Development of Jiangsu Higher Education Institutions (PAPD) and the program of Innovative Research Team of Changzhou University (ZMF1002118) are gratefully acknowledged.

References

[1] Ganivada MN, Rao NV, Dinda H, Kumar P, Sarma JD, Shunmugam R. Macromolecules 2014;47;2703-11.

[2] Zhao XB, Liu P. Mol Pharmaceutics 2014;11;1599-610.

[3] Du AW, Stenzel MH. Biomacromolecules 2014;15;1097-114.

[4] Blunden BM, Rawal A, Lu HX, Stenzel MH. Macromolecules 2014;47;1646-1655.

[5] Meng FH, Zhong ZY, Feijen J. Biomacromolecules 2009;10;197-209.

[6] Gong YH, Li C, Yang J, Wang HY, Zhuo RX, Zhang XZ. Macromolecules 2011;44;7499-502.

[7] Sun W, Zhou SX, You B, Wu LM. Macromolecules 2013;46;7018-26.

[8] Qing GY, Wang X, Fuchs H, Sun TL. J Am Chem Soc 2009;131;8370-71.

[9] Hong CY, Li X, Pan CY. J Phys Chem C 2008;112;15320-24.

[10] Yan Q, Zhang HJ, Zhao Y. ACS Macro Lett 2014;3;472-6.

[11] Zhang ZK, Ma RJ, Shi LQ. Acc Chem Res 2014;47;1426-37.

[12] Lee SM, Nguyen ST. Macromolecules 2013;46;9169-80.

[13] Han XG, Liu YD, Yin YD. Nano Lett 2014;14;2466-70.

[14] Lin YA, Xia XX, Wang M, Wang QR, An B, Tao H, Xu QB, Omenetto,F, Kaplan DL. Langmuir 2014;30;4406-14.

[15] Hiruta Y, Shimamura M, Matsuura M, Maekawa Y, Funatsu T, Suzuki Y, Ayano E, Okano T, Kanazawa H. ACS Macro Lett 2014;3;281-5.

[16] Shao H, Wang CF, Zhang J, Chen S. Macromolecules 2014;47;1875-81.

[17] Nagase K, Kobayashi J, Kikuchi A, Akiyama Y, Kanazawa H, Okano T. Biomacromolecules 2014;15;1204-15.

[18] Nagase K, Kobayashi J, Kikuchi A, Akiyama Y, Kanazawa H, Okano T. ACS Appl Mater Interfaces 2012;4;1998-2008.

[19] Xue XQ, Li F, Huang WY, Yang HJ, Jiang BB, ZhengYL, Zhang DL, Fang JB, Kong LZ, Zhai GQ, Chen JH. Macromol Rapid Commun 2014;35;330-6.

[20] Wang Y, Li X, Hong CY, Pan CY. J Polym Sci Part A: Polym Chem 2011;49;3280-90.

[21] Tian HY, Yan JJ, Gu C, You YZ, Chen XS. Macromol Rapid Commun 2011;32;660-4.

[22] Schild HG. Prog Polym Sci 1992;17;163-249.

[23] Leduc MR, Hawker CJ, Dao J, Frechet JMJ. J Am Chem Soc 1996;118;11111-7.

[24] Nuopponen M, Ojala J, Tenhu H. Polymer 2004;45;3643-50.

[25] Zheng YJ, Li GL, Deng HP, Su Y, Liu JH, Zhu XY. Polym Chem 2014;5;2521-9.

[26] Sun ST, Wu PY. Soft Matter 2011;7;7526-31.

[27] Zhang WD, Zhang W, Cheng ZP, Zhou NC, Zhu J, Zhang ZB, Chen GJ, Zhu XL. Macromolecules 2011;44;3366-73.

[28] Andre X, Zhang MF, Muller AHE. Macromol Rapid Commun 2005;26;558-63.

[29] Sun WQ, He XH, Gao CY, Liao XJ, Xie MR, Lin SL, Yan DY. Polym Chem 2013;4;1939-49.

[30] Zhang X, Yang PP, Dai YL, Ma PA, Li XJ, Cheng ZY, Hou ZY, Kang XJ, Li CX,

Lin J. Adv Funct Mater 2013;23;4067-78.

[31] Zhao Y, Shi XB, Gao HY, Zhang L, Zhu FM, Wu Q. J Mater Chem 2012;22;5737-45.

[32] Wong JE, Díez-Pascual AM, Richtering W. Macromolecules 2009;42;1229-38.

[33] Men YJ, Drechsler M, Yuan JY. Macromol Rapid Commun 2013;34;1721-27.

[34] Dai S, Ravib P, Tam KC. Soft Matter 2009;5;2513-33.

[35] Yin J, Hu HB, Wu YH, Liu SY. Polym Chem 2011;2;363-71.

[36] Yu YY, Tian F, Wei C, Wang CC. J Polym Sci Part A: Polym Chem 2009;47;2763-73.

[37] Mu B, Liu P, Li XR, Du PC, Dong Y, Wang YJ. Mol Pharmaceutics 2012;9;91-101.

[38] Snowden MJ, Chowdhry BZ, Vincent B, Morris GE. J Chem Soc Faraday Trans 1996;92;5013-6.

[39] Rahane SB, Floyd JA, Metters AT, Kilbey SM. Adv Funct Mater 2008;18;1232-40.

[40] Kumar G, Neckers DC. Chem Rev 1989;89;1915-37.

[41] Delaire JA, Nakatani K. Chem Rev 2000;100;1817-45.

[42] Natansohn A, Rochon P. Chem Rev 2002;102;4139-75.

[43] Gibons WM, Shannon PJ, Sun ST, Swetlin BJ. Nature 1991;351;49-50.

[44] Rochon P, Batalla E, Natansohn A. Appl Phys Lett 1995;66;136-8.

[45] Kim DY, Tripathy SK, Li L, Kumar J. Appl Phys Lett 1995;66;1166-8.

[46] Xue XQ, Zhu J, Zhang ZB, Zhou NC, Tu YF, Zhu XL. Macromolecules 2010;43;2704-12.

[47] Hafiz HR, Nakanishi F. Nanotechnology 2003;14;649-54.

[48] Tong X, Cui L, Zhao Y. Macromolecules 2004;37;3101-12.

[49] Rasmussen PH, Ramanujam PS, Hvilsted S, Berg RH. J Am Chem Soc 1999;121;4738-43.

[50] Kumar KRS, Kamei T, Fukaminato T, Tamaoki N. ACS Nano 2014;8;4157-65.

[51] Jin Q, Liu GY, Liu XS, Ji J. Soft Matter 2010;6;5589-95.

[52] Wang DR, Ren HF, Wang XQ, Wang XG. Macromolecules 2008;41;9382-8.

[53] Wang G, Tong X, Zhao Y. Macromolecules 2004;37;8911-7.

[54] Blasco E, Schmidt BVKJ, Barner-Kowollik C, Piñol M, Oriol L. Macromolecules 2014;47;3693-700.

[55] Kungwatchakun D, Irie M. Makromol Chem Rapid Commun 1988;9;243-6.

[56] Feng Z, Lin L, Yan Z, Yu YL. Macromol Rapid Commum 2010;31;640-4.

[57] Ueki T, Nakamura Y, Yamaguchi A, Niitsuma K, Lodge TP, Watanabe M. Macromolecules 2011;44;6908-14.

[58] Ueki T, Nakamura Y, Lodge TP, Watanabe M. Macromolecules 2012;45;7566-73.

[59] Jochumab FD, Theato P. Chem Soc Rev 2013;42;7468-83.

[60] Boissiere O, Han D, Tremblay L, Zhao Y. Soft Matter 2011;7;9410-5.

[61] Liu YJ, Pallier A, Sun J, Rudiuk S, Baigl D, Piel M, Mariea E, Tribet C. Soft Matter 2012;8;8446-55.

[62] Liu JH, Chen GS, Guo MY, Jiang M. Macromolecules 2010;43;8086-93.

[63] He J, Tremblay L, Lacelle S, Zhao Y. Polym Chem 2014;5;5403-11.

[64] Akiyama H, Tamaoki N. Macromolecules 2007;40;5129-32.

[65] Jochum FD, Borg LZ, Roth PJ, Theato P. Macromolecules 2009;42;7854-62.

[66] Yu B, Jiang XS, Wang R, Yin J. Macromolecules 2010;43;10457-65.

[67] Zhang J, Liu HJ, Yuan Y, Jiang SZ, Yao YF, Chen Y. ACS Macro Lett 2013;2;67-71.

[68] Patterson JP, Kelley EG, Murphy RP, Moughton AO, Robin MP, Lu A, Colombani O, Chassenieux C, Cheung D, Sullivan MO, Epps TH, O'Reilly RK. Macromolecules 2013;46;6319-25.

[69] Ciampolini M, Nardi N. Inorg Chem 1966;5;41-4.

[70] Xue XQ, Zhu J, Zhang ZB, Cheng ZP, Tu YF, Zhu XL. Polymer 2010;51;3083-90.

[71] Akiyama H, Tamaoki N. J Polym Sci., Part A: Polym Chem 2004;42;5200-14.

[72] Israelachvili JN. In Intermolecular and Surface Forces, 3rd ed, Academic Press: Amsterdam, 2011; Part III p 536, 539.

[73] Burchard W. Adv Polym Sci 1999;143;113-94.

[74] Wu C, Li M, Kwan S, Liu G. Macromolecules 1998;31;7553-4.

[75] Niu AZ, Liaw DJ, Sang HC, Wu C. Macromolecules 2000;33;3492-4.

Highlights

LCST for the 4-propoxyazobenzene-terminated PNIPAM solution clearly decreased after UV irradiation, and the repeated LCST difference depended on both the number-average molecular weight and amount of azobenzene chromophore. The PNIPAM solution could self-assemble into nano-micelles with 4-propoxyazobenzene as the hydrophobic cores and PNIPAM chains as the hydrophilic shells. After UV irradiation, the unstable spherical micelles transformed to metastable nanorods, then to longer rods, and finally to flake-like particles via horizontal inter-rod aggregation by heating, which led to the LCST downshift.

Temperature-Light Dual Stimuli-Responsive Nanorods from Self-Assembly of the 4-Propoxyazobenzene-Terminated Poly(*N*-isopropylacrylamide) in Aqueous Solution

Xiaoqiang Xue, Jing Yang, Wenyan Huang, Hongjun Yang, Bibiao Jiang*, Fang Li

Jiangsu Key Laboratory of Material Surface Science and Technology, School of Material Science and Engineering, Changzhou University, Changzhou, Jiangsu, 213164, People's Republic of China

Synthesis of the 4-propoxyazobenzene-terminated poly(*N*-isopropylacrylamide) (PNIPAMs) via the atom transfer radical polymerization (ATRP). Firstly, the hydrophobic 4-propoxyazobenzene-containing compounds (4-propoxy-4′-(2-bromopropionyloxy)azobenzene, PAzo-Br) as ATRP initiator was successfully obtained from sequential multiple-step reaction, *i.e.* alkylation, nitrobenzene reduction, diazonium, azo-coupling and esterification reaction in Scheme S1. The structure of PAzo-Br was characterized by ^{1}H NMR spectrum (Figure S1).

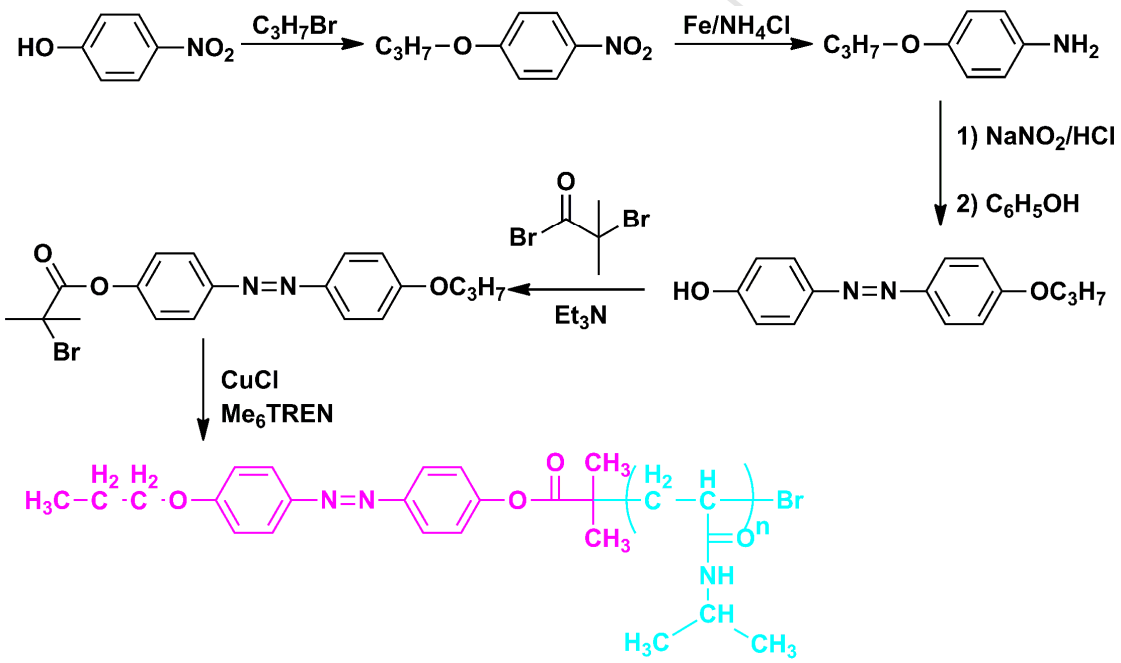

Scheme S1. Synthetic Route of the 4-propoxyazobenzene-terminated poly(*N*-isopropylacrylamide) (PNIPAM).

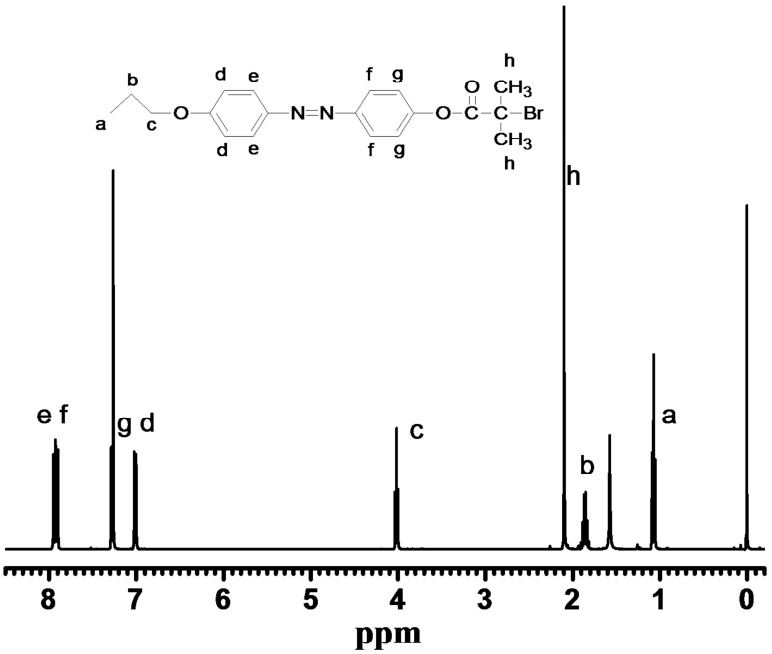

Figure S1. ^{1}H NMR spectrum of 4-propoxy-4′-(2-Bromopropionyloxy)azobenzene (PAzo-Br) in $CDCl_3$.

Secondly, PNIPAM with the end functional group was easily synthesized by ATRP employing functional initiator so as to produce the end group. PAzo-Br as the ATRP initiator could be used for the ATRP of (meth)acrylate monomers, because of the formation and incorporation of radical efficiently into the poly(meth)acrylate propagating chain.[1] Generally speaking, ATRP of acrylamides has undergone lack of control and low conversions due to the competitive coordination of their amide groups with the metal catalysts. Tris[2-(dimethylamino)ethyl]amine (Me_6TREN)[2] as the efficient ligand improves extensive catalyst activation, and highly polar solvents[3] such as

alcohol, water, *N*, *N*-dimethylformamide, etc. as polymerization solvents can protect the catalyst by hydrogen bonding to the amide groups of both monomer and polymer. Moreover, the mixed halogen initiating system (R-Br/CuCl)[4] has been previously used to improve the control of ATRP. Therefore, ATRP of NIPAM using PAzo-Br initiator was carried out using isopropyl alcohol:water = 2:1 (m/m) as polymerization solvents at 25 ^{o}C and several molar ratios of chemicals as follows: $[NIPAM]_0$:$[PAzo\text{-}Br]_0$:$[CuCl]_0$:$[Me_6TREN]_0$ = 30~90:1:1:3. The results of several polymerizations with different molar ratios are shown in Table S1. A series of PNIPAMs with the different molecular weights were successfully prepared by varying molar ratios of components and the polymerization time. The measured number-average molecular weights ($M_{n\,GPC}$s) of PNIPAMs ranged from 3100 to 15000 g mol^{-1} while still keeping the relatively narrow molecular weight distributions (M_w/M_n < 1.35), which indicated that the polymerization was conducted under a controlled manner. The GPC traces (Figure S2) of PNIPAMs showed an almost symmetric peak with no tailing or shoulder at the lower or higher molecular weight side, indicating a negligible premature chain termination and high end-functionalized degrees of polymers.

Table S1. Characteristic data for polymers (PNIPAM1~PNIPAM7).

Sample[a]	$[NIPAM]_0$:$[PAzo\text{-}Br]_0$:$[CuCl]_0$:$[Me_6TREN]_0$[b]	time[c] (h)	*Conv.*[d] (%)	$M_{n\ GPC}$[e] (g mol^{-1})	M_w/M_n[e]	$M_{n\ th}$ (g mol^{-1})	$M_{n\ NMR}$[f] (g mol^{-1})	LCST[g] (^oC)
PNIPAM1	30:1:1:3	4	64.18	3100	1.20	2600	2800	30.4
PNIPAM2	30:1:1:3	5	70.98	3900	1.35	2800	3200	30.3
PNIPAM3	30:1:1:3	7	80.20	4400	1.29	3100	3500	29.3
PNIPAM4	30:1:1:3	10	90.06	5300	1.16	3400	4100	29.0
PNIPAM5	60:1:1:3	8	88.21	8100	1.35	6300	7100	29.3
PNIPAM6	60:1:1:3	12	95.56	10800	1.31	6800	9000	32.4
PNIPAM7	90:1:1:3	10	80.12	15000	1.27	8500	13100	33.3

[a] 4-Propoxyazobenzene-terminated poly(*N*-isopropylacrylamide)s (PNIPAMs) were synthesized via atom transfer radical polymerization (ATRP) of *N*-isopropylacrylamide (NIPAM) using 4-propoxy-4'-(2-bromopropionyloxy)azobenzene (PAzo-Br) as ATRP initiator, CuCl/tris[2-(dimethylamino)ethyl]amine (Me_6TREN) as catalytic system and isopropyl alcohol/water (2:1, m/m) as mix solvents at 25 ^oC. [b] Typically 1.13 g of NIPAM (10 mmol). [c] Polymerization time. [d] Conversion determined by an HP-689 gas chromatography equipped with an HP-5 column (30m×0.54mm×0.5μm). Isopropyl alcohol was used as the internal standard. [e] Determined by gel permeation chromatography (GPC) using tetrahydrofuran (THF) as the eluent. M_n: the number-average molecular weight. M_w: the weight-average molecular weight. M_w/M_n: molecular weight distribution. [f] The number-average molecular weight measured by ^1H NMR according to eq 1. [g] Lower critical solution temperature (LCST) of polymer solution (2 mg mL^{-1}) in water was determined by optical transmittance of a 550 nm light versus the temperature using an Agilent Cary 100 equipped with a Cary dual cell peltier accessory (Varian).

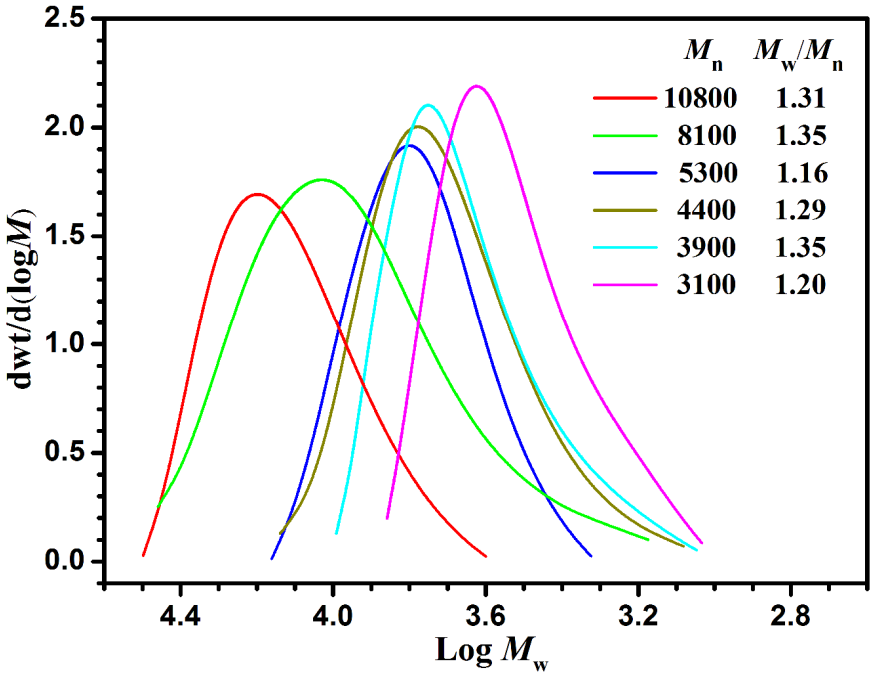

Figure S2. Overlay of GPC curves of the 4-propoxyazobenzene-terminated Poly(*N*-isopropylacrylamide)s

To confirm the polymer structures with the end functional group, the obtained polymer was characterized by ^{1}H-NMR spectrum. As shown in Figure S3, the characteristic signals at 3.85-4.27 ppm (c in Figure S3) were assigned to the methenyl protons of the NIPAM units. The signals at approximately 0.72-2.77 ppm were ascribed to other alkyl protons of the NIPAM units. Moreover, the chemical shifts at around 7.82-7.98 ppm (a in Figure S3) were due to phenyl protons of the azobenzene group in the end of PNIPAM, and the signals attributed to other phenyl protons of the azobenzene connected to the substituents were observed at about 6.95-7.06 ppm, which confirmed

the existence of the PAzo-Br moiety at the end of the polymer chains. The molecular weights of the PNIPAMs ($M_{n\ NMR}$s) could be estimated according to the integrals calculated by ^{1}H NMR spectra, and given by eq 1:

$$M_{n\ NMR} = \frac{I_{3.85\text{ - }4.27} - I_{7.82\text{ - }7.98}/2}{I_{7.82\text{ - }7.98}/4} \times M_{NIPAM} + M_{PAzo\text{-}Br} \qquad (1)$$

Where, $I_{3.85\text{-}4.27}$ and $I_{7.82\text{-}7.98}$ were the integrals of the signals at 3.85-4.27 ppm and 7.82-7.98 ppm in Figure S3, respectively. The characteristic signals of the methylene protons from the terminal 4-propoxyazobenzene were overlapped by the methenyl protons of the NIPAM units. Therefore, the integral of the NIPAM units had been changed to $I_{3.85\text{-}4.27} - I_{7.82\text{-}7.98}/2$. As summarized in Table S1, the results showed that the $M_{n\ NMR}$ was smaller than the corresponding $M_{n\ GPC}$ for each PNIPAM, which may be due to the difference of hydrodynamic volumes between the PNIPAMs and linear PS standards, and the $M_{n\ NMR}$s as revealed by ^{1}H NMR gave the reliable results because of the high end-functionalized degrees of polymers obtained by ATRP.[2,3]

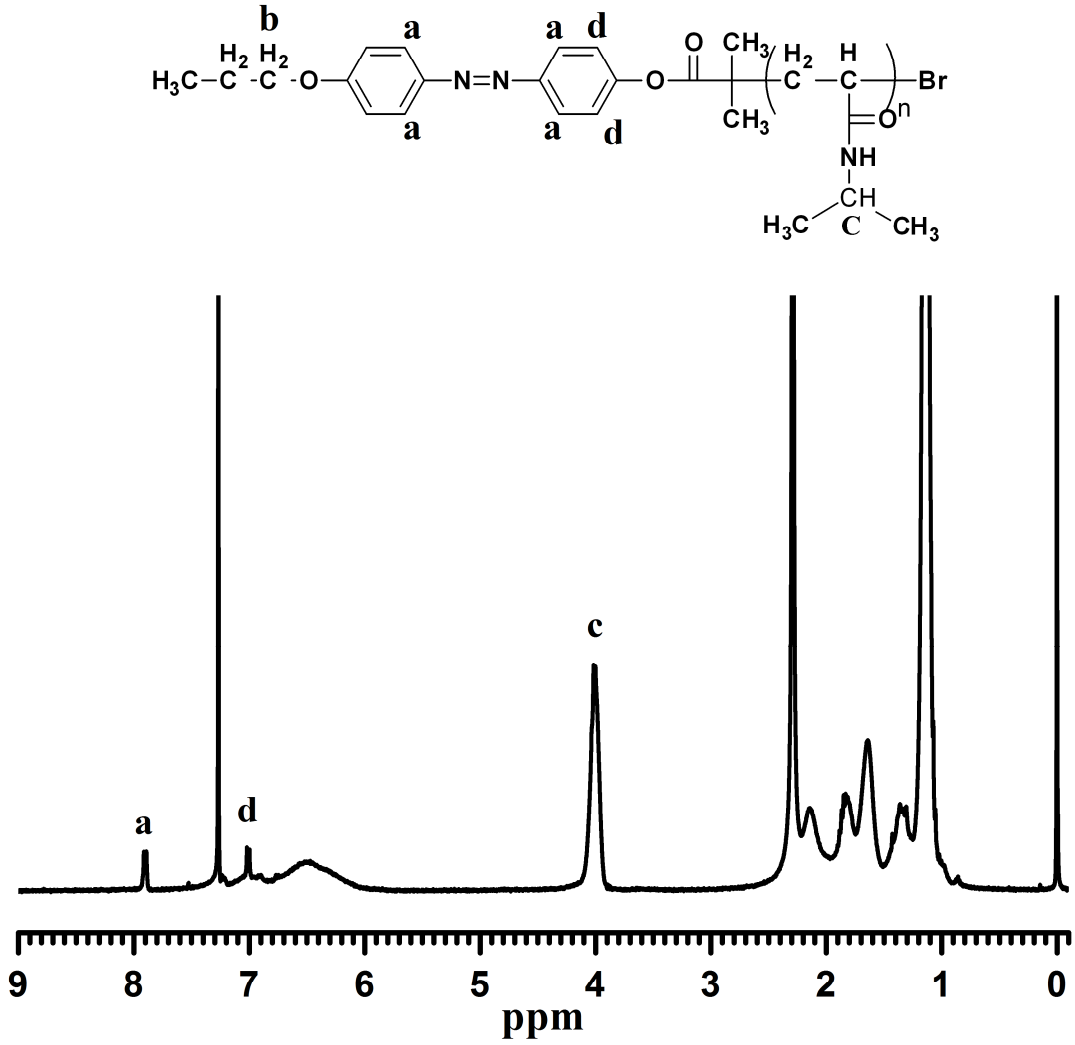

Figure S3. ^{1}H NMR spectrum of the PNIPAM4 ($M_{n\,GPC}$ = 5300 g mol^{-1}, M_w/M_n = 1.16) in $CDCl_3$

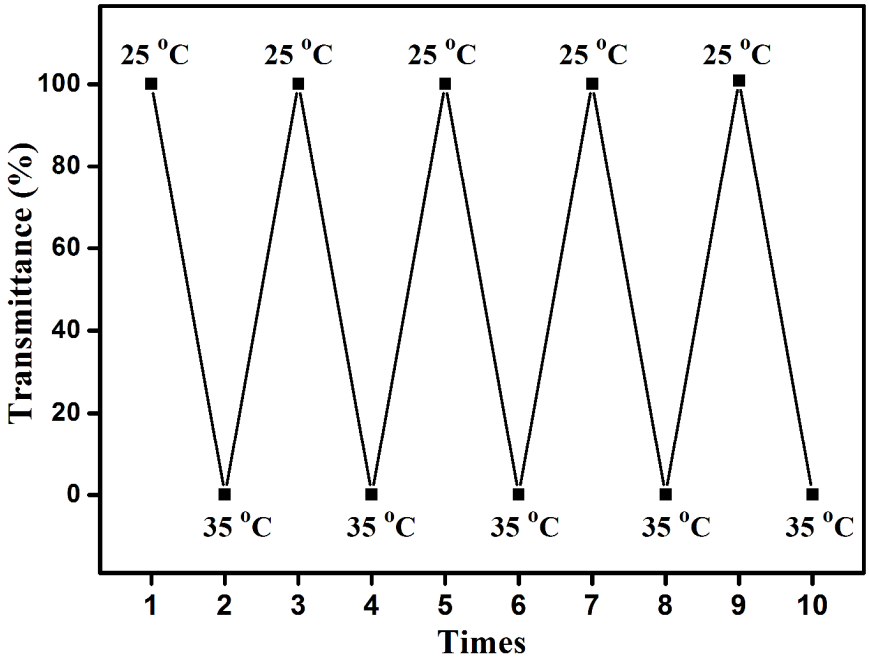

Figure S4. Reversible changes of transmittance at 550 nm for the PNIPAM4 ($M_{n\ GPC}$ = 5300 g/mol, M_w/M_n = 1.16) aqueous solution (2 mg mL^{-1}) at alternating temperatures of 25 °C and 35 °C.

(1) Matyjaszewski, K.; Tsarevsky, N. V. *J. Am. Chem. Soc.* **2014**, *136*, 6513-6533.

(2) Neugebauer, D.; Matyjaszewski, K. *Macromolecules* **2003**, *36*, 2598-2603.

(3) Xia, Y.; Yin, X. C.; Burke, N. A. D.; Stö1ver, H. D. H. *Macromolecules* **2005**, *38*, 5937-5943.

(4) Matyjaszewski, K.; Shipp, D. A.; Wang, J. L.; Grimaud, T.; Patten, T. E. *Macromolecules* **1998**, *31*, 6836-6840.